RESEARCH ARTICLE

Figures and figure supplements

Rapid, DNA-induced interface swapping by DNA gyrase

Thomas RM Germe *et al*.

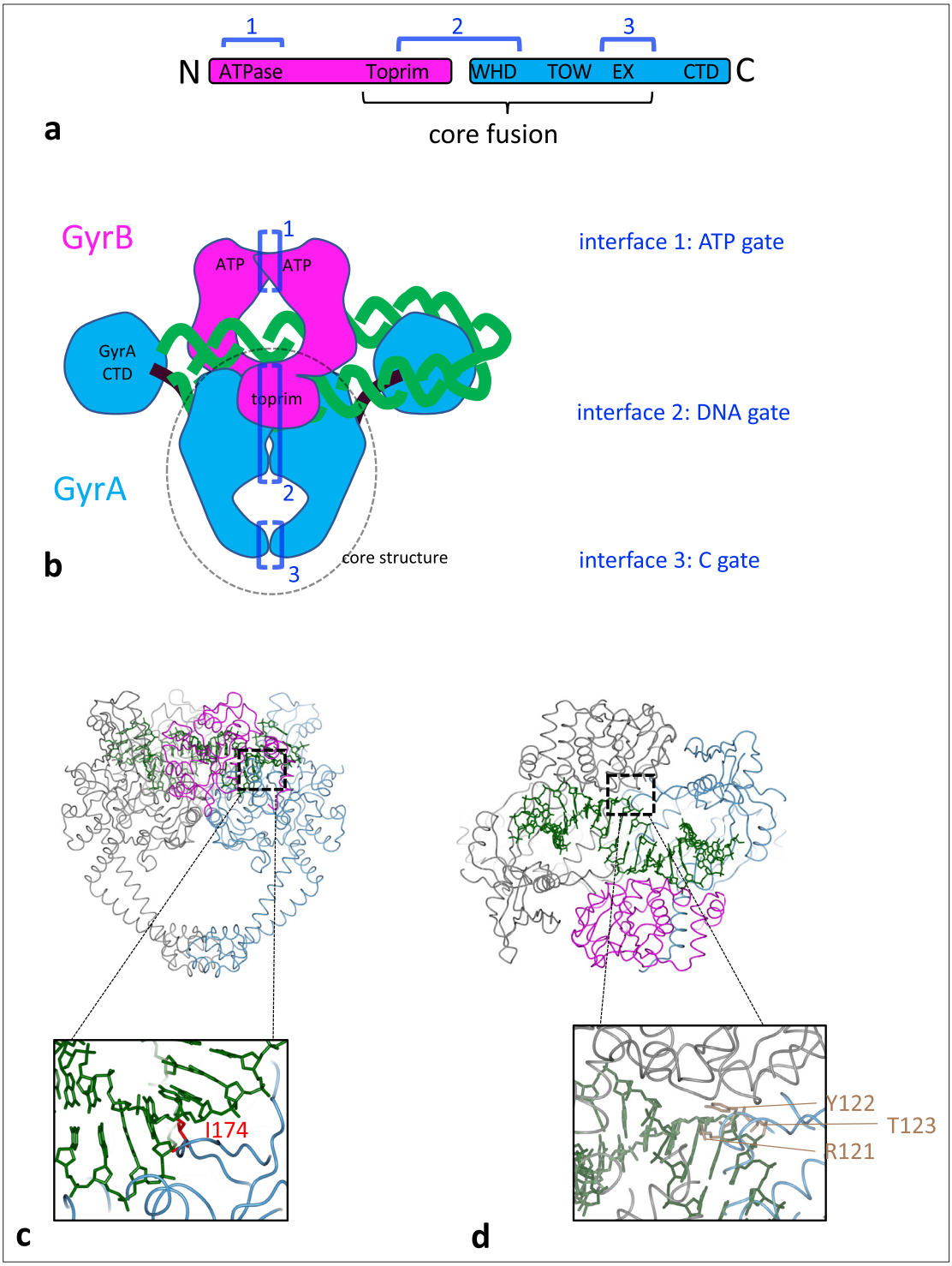

Figure 1. Structural organisation of DNA gyrase. (**a**) Schematic of DNA gyrase peptidic sequences. GyrB is in purple and GyrA in blue. The core fusion construct used in structural studies is indicated. The sequences engaging in one of the three interfaces are indicated by dark blue brackets. (**b**) Cartoon rendering of the DNA gyrase heterotetramer, color-coded as above. The part of the enzyme included in the *S. aureus* core fusion structure is circled with a dashed line. Various domains are indicated, and the three interfaces the transported DNA go through are are labeled 1–3 in the order of passage. (**c**) Side view of *S. aureus* DNA gyrase core fusion structure (6FQV) with bound DNA (green) (only the TOPRIM domain here). The C2 symmetry mate is rendered in gray. The inset shows the location of isoleucine 174 in red (*E. coli* numbering) which is inserted between base +8 and+9 (from scissile phosphate) and introduces a kink in the duplex. (**d**) Top view of the same structure. The inset shows in light brown the catalytic tyrosine sandwiched between an arginine and a threonine and forming the triad RYT.

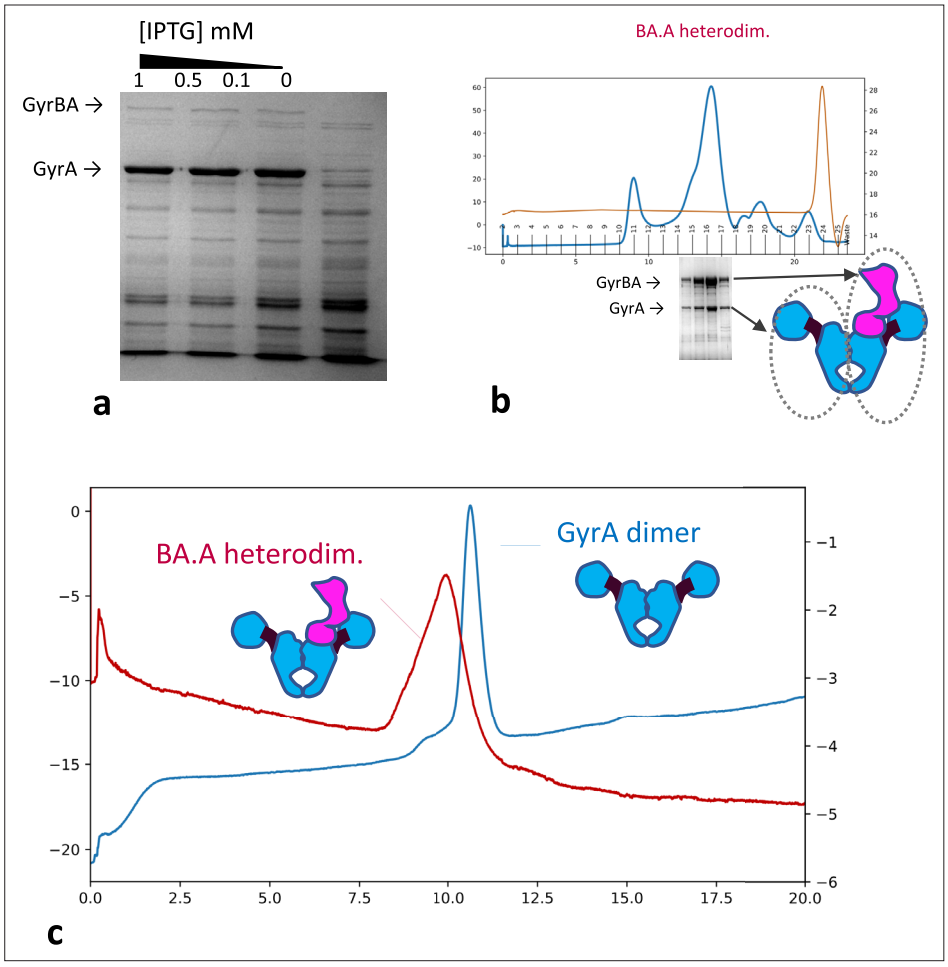

Figure 1—figure supplement 1. Gel filtration and SDS-PAGE analysis of our heterodimer preparation. (**a**) Co-expression of GyrBA fusion and GyrA in *E. coli*. GyrA is expressed at a much higher level compared to GyrBA, thereby favouring the formation of BA.A heterodimers and A_2 dimers. (**b**) Last polishing step of the heterodimer preparation; the preparation is passed through a Superose 6 column. The abscissa is the elution volume. In blue is the UV absorbance in arbitrary units; in brown is the conductivity (the salt peak indicates the total column volume). The fractions are indicated at the bottom. Fractions 10–20 contain the heterodimer complex and are analyzed by SDS-PAGE (bottom) stained with Coomassie. The GyrA and GyrBA fusion bands are indicated. (**c**) Analytical gel filtration of BA.A (red line) compared to a GyrA sample (blue line); an analytical Superdex 200 column was used, BA.A and GyrA form distinct peaks. The GyrA peak elutes at around 160 kDa (compared to a native marker) and the BA.A heterodimer at around 180–190 kDa, much lower than its theoretical MW.

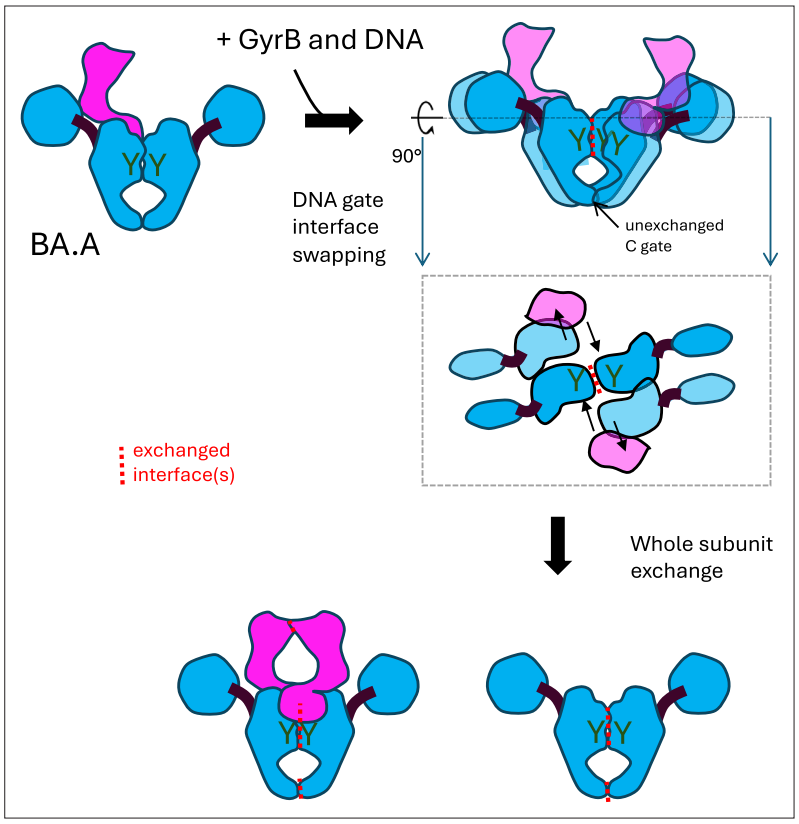

Figure 1—figure supplement 2. Schematic of possible sequential interface swapping mechanism leading to complete subunit exchange. Top left, schematic of the BA.A heterodimer. Two heterodimers having undergone DNA gate interface swapping are represented Top Right. The exchanged interfaces are shown with the red dashed line. The dashed black line represents a plane intersecting the swapped heterodimer horizontally. Just below the Top Right schematic is a view from the top of this plane and any elements outside the plane is excluded. Bottom. Subsequent exchange of the C gate and the N gate produces two exchanged dimers (A_2 and BA_2) from the original 2 BA.A heterodimer. The approximate position of the catalytic tyrosine (Y in dark green) is indicated.

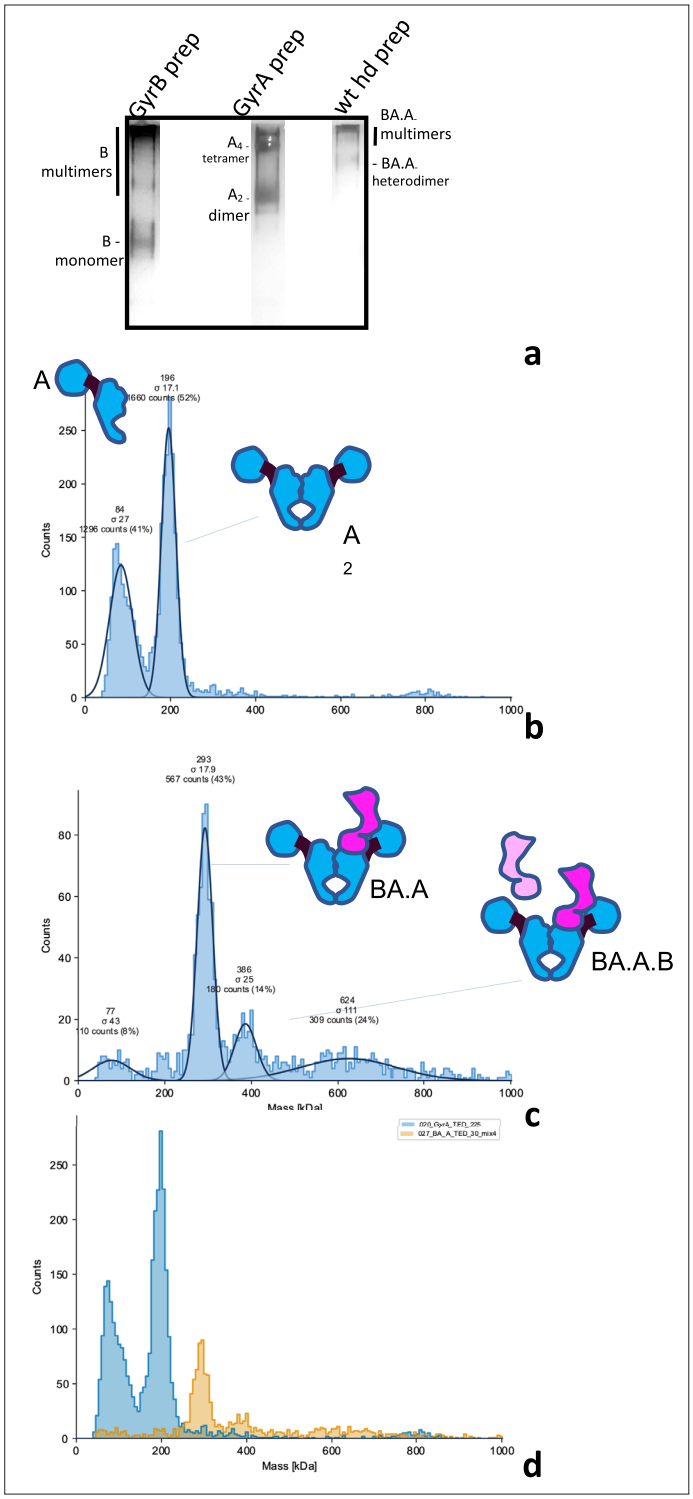

Figure 2. Analysis of GyrA, GyrB, and heterodimers preparations. (**a**) Blue-Native PAGE of our GyrB, GyrA and wild-type heterodimer preparation. The bands constituted by GyrB monomers, GyrA dimers and heterodimers are indicated and were visualized by silver staining. The migration pattern was ascertained by comparison to a native marker and is consistent with mass photometry profiles below. (**b**) Mass Photometry profile of the GyrA preparation. The histogram shows the counts of collisions events plotted against the scattering intensity, which is proportional to the MW and is calibrated against urease; the abscissa shows the molecular mass in kDa. The instrument fits the observed peaks to gaussian curves (continuous black lines) and the mean (MW) and deviation (σ) of the fitted curves are indicated on top of the peak, alongside the total count for the peak and the percentage

Figure 2 continued on next page

Figure 2 continued

of counts assigned to the peak with respect to the total number of fitted events. (**c**) Mass Photometry profile of our wild-type heterodimer preparation, as above. Note that the lower the peak count, the higher the deviation. We detect a main peak at approximately the expected size for a heterodimer. (**d**) Superimposition of the two profiles (GyrA dimer in blue and heterodimer in orange) showing the difference in mass between the heterodimer and the GyrA dimer. The two profiles were collected on the same day, in the same buffer and with the same calibration.

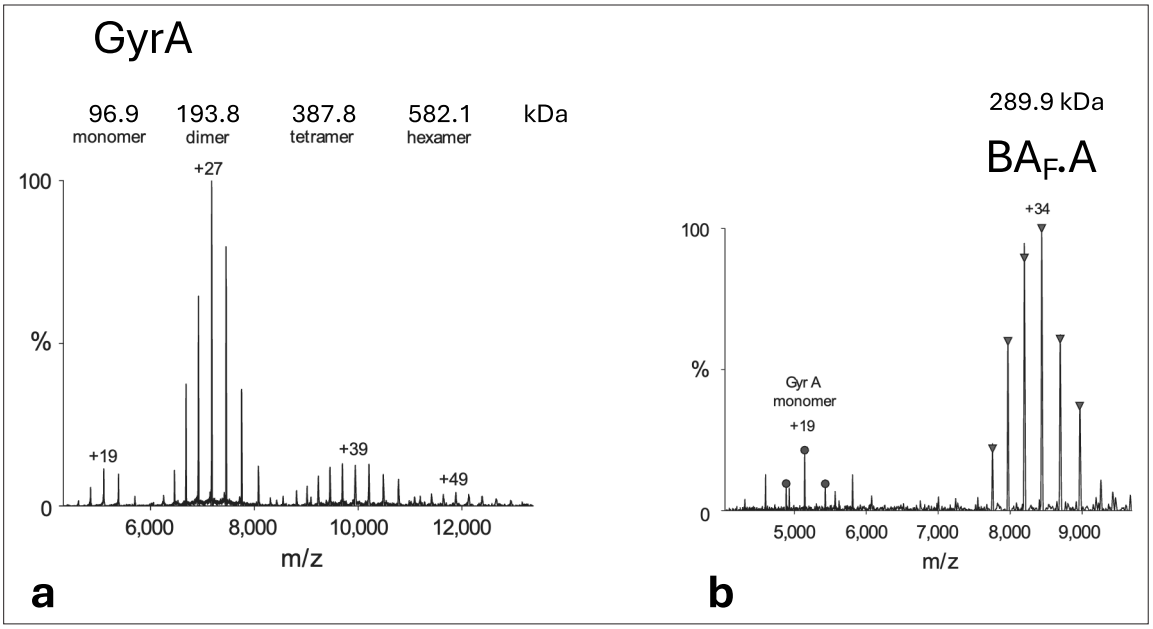

Figure 2—figure supplement 1. Analysis of GyrA and $BA_F.A$ preparation by native mass spectrometry. (**a**) GyrA. The preparation resolves into four peaks with Molecular Weights (MWs) consistent for the GyrA monomer, dimer, tetramer, and hexamer. Measured MWs are indicated in kDa. The theoretical MW of the GyrA monomer is 96,947 Da. (**b**) $BA_F.A$. The preparation resolves into two peaks, with some impurities at around 60 kDa. The measured MW of $BA_F.A$ is indicated in kDa. The theoretical MW of $BA_F.A$ is 285,847 Da. The numbers indicate the ionization state of the most intense peak.

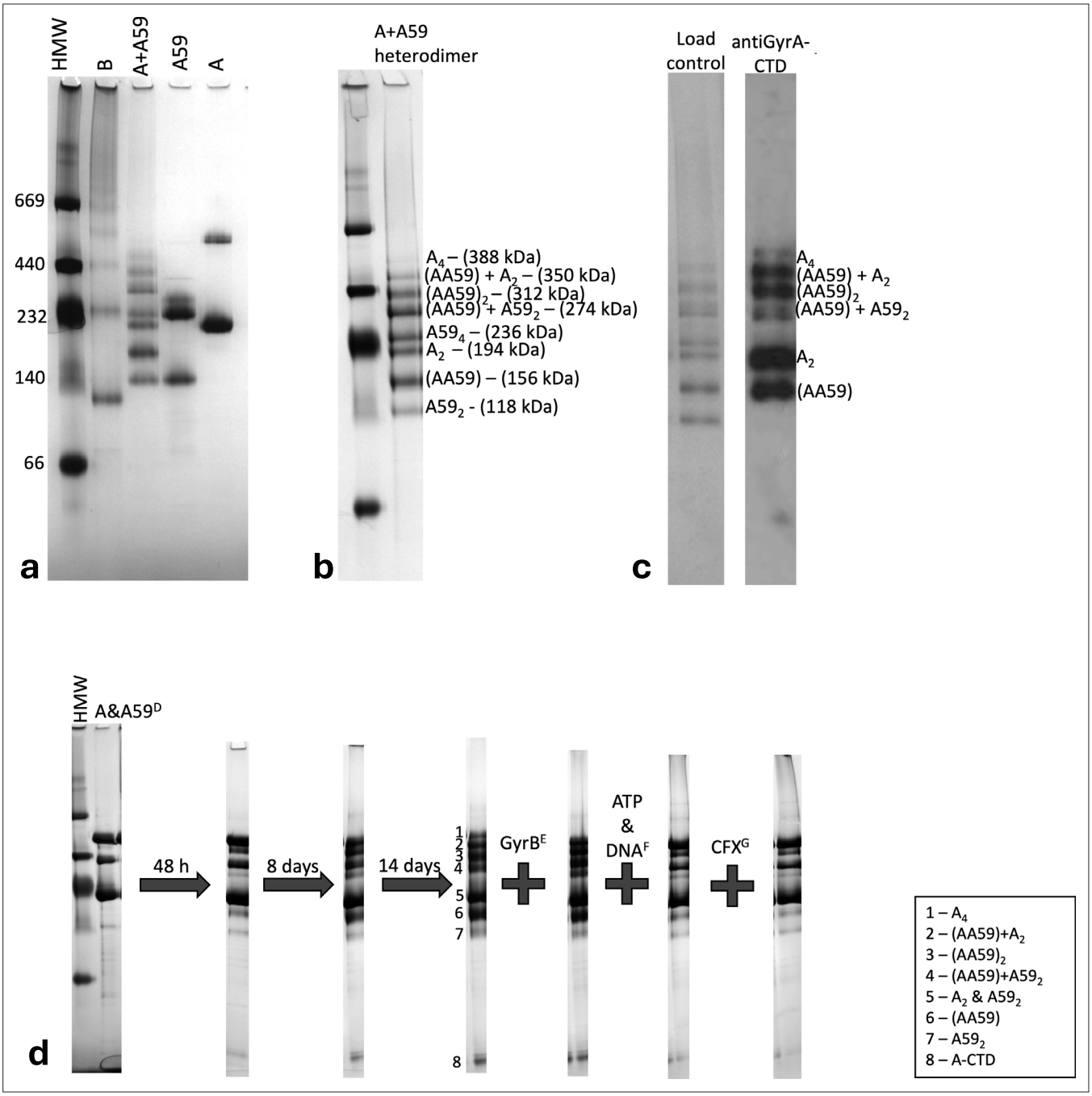

Figure 2—figure supplement 2. Blue-Native PAGE and western blot of the GyrA/GyrA59 heterodimers. (**a**) BN-PAGE GyrA (A), $GyrA_{59}$ (A59), a refolded heterodimer (A+A59) and GyrB (B) run on a 4–12% gradient gel. HMW is the high molecular weight marker with the size of each band in kDa down the left-hand side. (**b**) Refolded heterodimer run as in **a** with the higher order complexes highlighted alongside, with their predicted molecular weights. (**c**) Refolded heterodimer run as in **a** stained with coomassie alongside the western blot probing for the GyrA-CTD. This antibody binds to full-length GyrA but not A_{59}. The bands were assigned on the basis of their reactivity with the antibody, combined with their molecular weight, estimated by comparison to the marker. A_4 is the GyrA tetramer, $A59_4$ is the GyrA59 tetramer, $(AA59)_2$ is the GyrA/GyrA59 heterotetramer, (AA59) is the heterodimer, A_2 is the GyrA dimer, $A59_2$ is the GyA59 dimer. (**d**) Effect of long-term incubation on subunit exchange. The A&A59 sample is run as in **a** after incubation for the indicated length of time, up to 14 days. 1–8 indicate the GyrA/GyrA59 complexes species. The arrow indicates the position of the heterodimer A.A59 (species 6). The last time point of the same experiment performed with the addition of GyrB, GyrB +ATP + DNA and GyrB +ATP + DNA+ciprofloxacin is shown on the right.

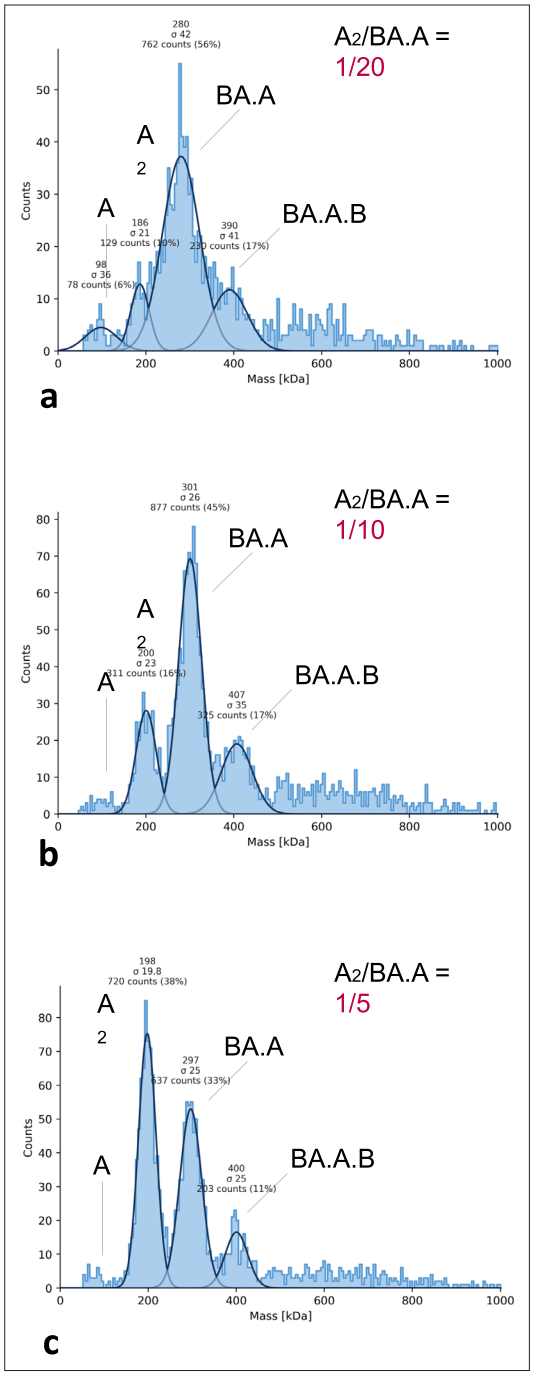

Figure 2—figure supplement 3. BA.A heterodimer and GyrA dimer mixing experiment; done to assess sensitivity of mass photometry to contaminating GyrA dimers mixed with BA.A heterodimers. 50 nM of BA.A were mixed with 2.5 nM (**a**), 5 nM (**b**) and 10 nM (**c**) of purified GyrA dimer. Data shows that 1/20 GyrA/BA.A contamination is detectable (**a**). Increasing this ratio drastically increases the count for the GyrA dimer peak to above the BA.A peak (**b and c**), despite the latter species being more abundant. This shows that the counts for each species is dependent not only on their abundance, but also how efficiently they collide to the

Figure 2—figure supplement 3 continued on next page

Figure 2—figure supplement 3 continued

surface. The intensity of peaks should not therefore be used as a measure of abundance.

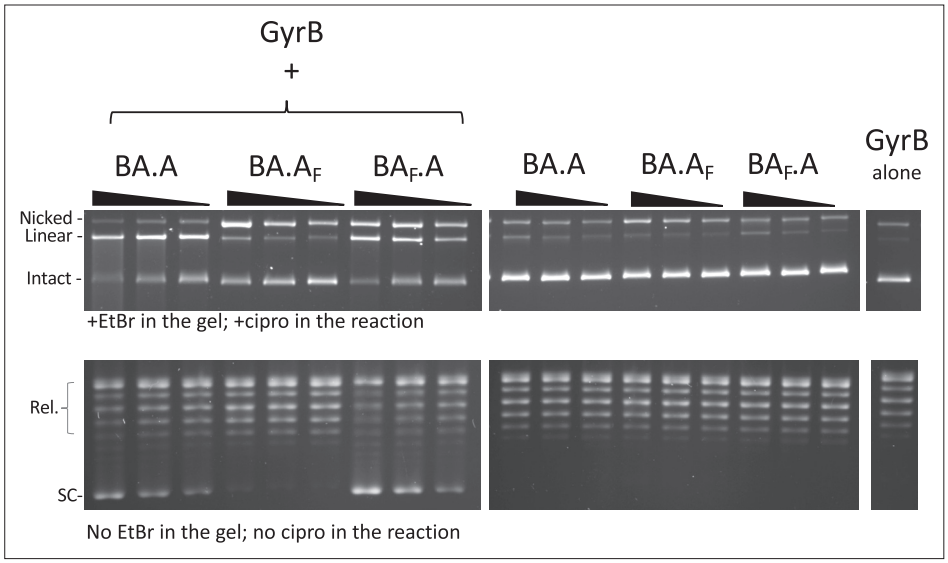

Figure 3. Reconstitution of double-strand cleavage activity in the presence of free GyrB. Both cleavage (top) and supercoiling (bottom) assays were performed with BA.A, BA.A$_F$ and BA$_F$.A as indicated. For cleavage assays, 5, 2.5, and 1.25 pmole of heterodimers (three lanes, from left to right for each heterodimer version, the triangle shows increasing dosage of heterodimers) were used. Eight pmole of GyrB were added to reconstitute the activity (top left panel). Omitting GyrB showed only background cleavage (top center panel). GyrB alone (top right panel) showed almost undetectable cleavage activity. For supercoiling assays, the dose of each subunit was reduced, so as to keep the activity limiting in the assay. Four pmole of GyrB was added to 1.25, 0.625, and 0.312 pmole of heterodimer, the triangle showing increasing dose of the heterodimer. Cleavage assays are analyzed with EtBr-containing agarose gels and the cleavage reaction contains 20 μM ciprofloxacin (cipro). Supercoiling assays do not contain cipro in the reaction and are analyzed on agarose gels that do not contain EtBr. The two types of gel/assay are indicated.

Figure 3—figure supplement 1. BA.A$_F$ can form double-strand cleavage complexes in the presence of GyrB. Five pmole of BA.A$_F$ were incubated in a cleavage assay in the presence of 8 pmole of GyrB. Control cleavage assays with BA.A$_F$ and GyrB alone were also performed. Cleavage complexes were purified and separated from naked DNA by phenol extraction (Supp. Methods). Protein-DNA adducts are trapped at the phenol interface and can be recovered (Phe). Naked DNAs remain in the aqueous phase (Aq). In the presence of GyrB, BA.A$_F$ produces mostly single-strand cleavage complexes, as expected. However, a significant minority of double-strand cleavage complexes are also recovered. The ** band is significantly more intense than the * band (as ascertained by densitometry) constituted by background double-strand cleavage complexes that occur with BA.A$_F$ alone (probably from contaminating GyrBA fusion dimers). The origin of these GyrB-induced double-strand cleavage complexes is discussed in the main manuscript. This experiment was reproduced three times with virtually identical results.

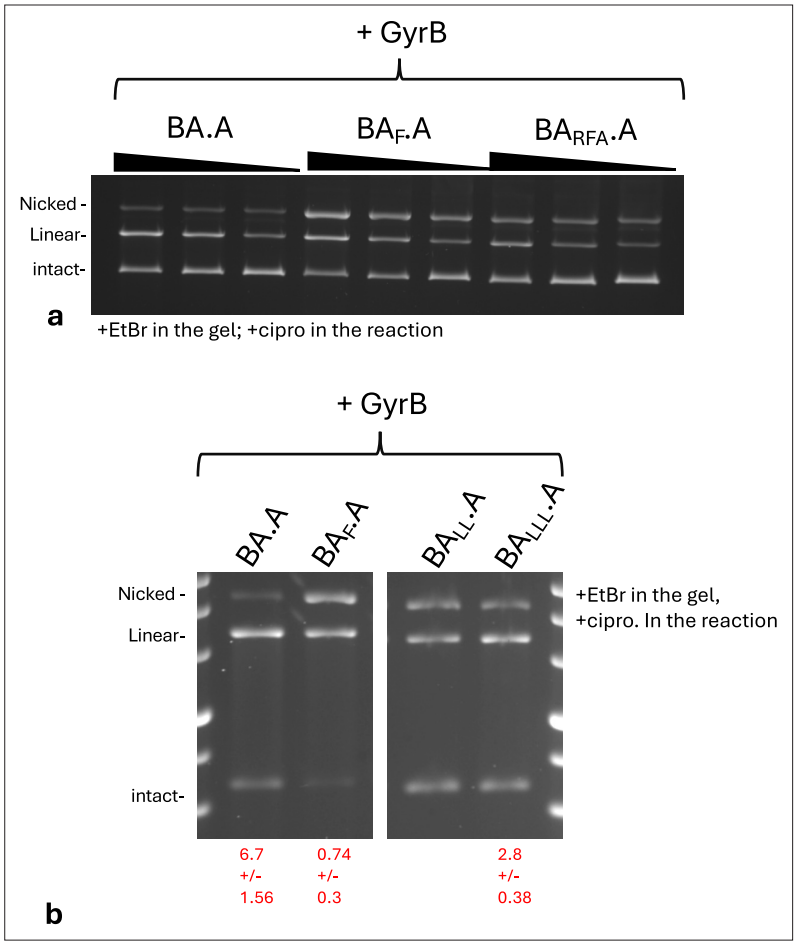

Figure 3—figure supplement 2. Cleavage activity of various heterodimer mutants. (**a**) 5, 2.5, and 1.25 pmole (triangle indicates increasing dose) of BA.A, BA$_F$.A and BA$_{FA}$.A (where the tyrosine adjacent to the catalytic tyrosine is mutated to an alanine) were incubated in a cleavage assay in the presence of GyrB. BA$_{FA}$.A displays significantly more double-strand to single-strand cleavage. (**b**) 5 pmole of BA$_F$.A, BA$_{LL}$.A and BA$_{LLL}$.A were tested as above. Again BA$_{LL}$.A and BA$_{LLL}$.A displayed higher double-strand cleavage activity (this is especially marked for BA$_{LLL}$.A). The double- to single-strand cleavage ratio is indicated in red with the standard deviation (unbiased) from three independent experiments.

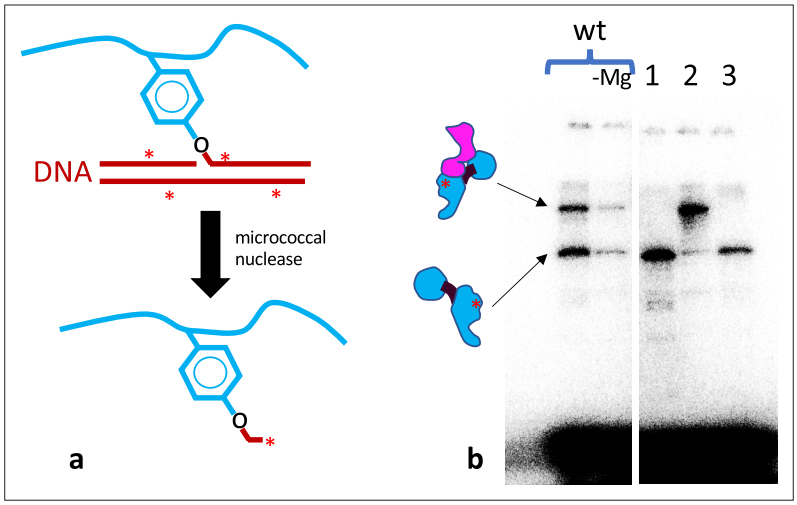

Figure 4. Labelling of the nucleophilic amino acid in gyrase. (**a**) Schematic of the radiolabeling of the catalytic tyrosine. The GyrA polypeptidic chain is schematized in blue, with the catalytic tyrosine shown. A cleavage reaction results in a covalent bond between the catalytic tyrosine and a radiolabeled DNA (in red with asterisks). Subsequent digestion with micrococcal nuclease digests most of the DNA and leaves a stub of radiolabeled nucleic acid covalently bound to the catalytic tyrosine. (**b**) The resulting labelled gyrase polypeptide can be analyzed by SDS-PAGE and detected by exposure to a phosphor screen. The cleavage reactions contained 8 pmole of GyrB and 5 pmole of heterodimer. From left to right: wild-type heterodimer with Mg^{2+}, without Mg^{2+}, BA_F.A (1), BA.A_F (2), and BA_{LLL}.A (3). The upper band is the fusion polypeptide, the lower band is the GyrA polypeptide. On both, the red asterisk shows the approximate position of the radioactive label. The smear at the bottom is the bulk of the digested radiolabeled DNA.

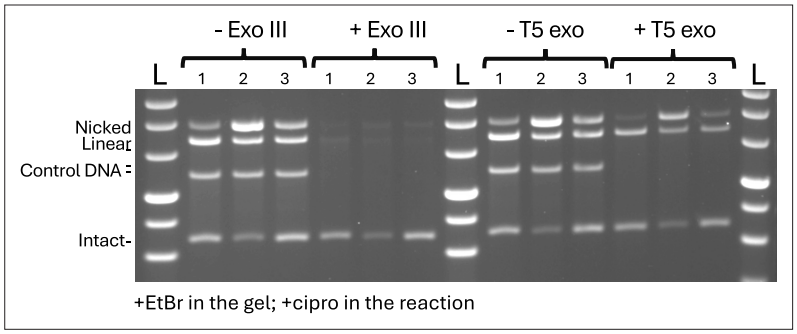

Figure 4—figure supplement 1. Exonuclease sensitivity of heterodimeric gyrase cleavage products. All reactions were performed with 5 pmole of heterodimer and 8 pmole of GyrB and purified before treatment (or not) with exonuclease as indicated. A purified PCR fragment was added to all reactions to control for nuclease activity (Control DNA). 1: BA.A (wild-type). 2: BA_{F}.A. 3: BA_{LLL}.A. L: Ladder.

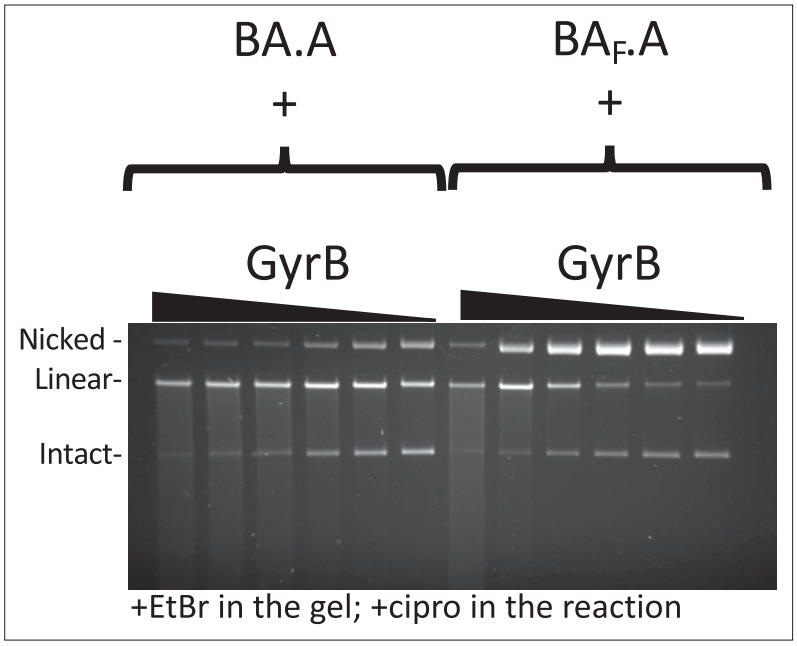

Figure 5. Effect of GyrB dose on subunit exchange. Five pmole of heterodimers (BA.A and BA$_F$.A as indicated) were incubated with increasing amounts of GyrB (triangle) in a cleavage assay. From the highest to the lowest dose: 16, 8, 4, 2, 1, and 0.5 pmole were used. At lower GyrB/heterodimer ratios, single-strand cleavage is predominant with BA$_F$.A, whereas BA.A still displays robust double-strand cleavage activity. Single-strand cleavage activity does go up marginally with the wild-type protein at the lower GyrB dose, suggesting missing GyrB on one side can lead to the formation of single-strand cleavage complexes. However, even at very low GyrB/heterodimer ratios, the majority of cleavage complexes are double-stranded.

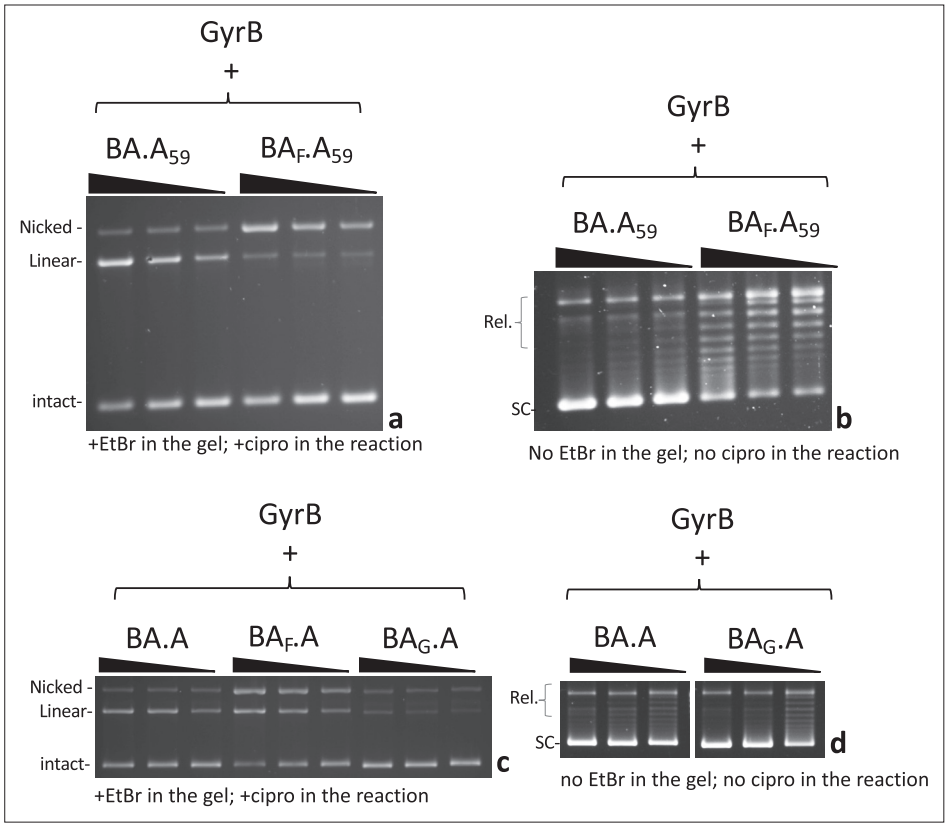

Figure 6. Effect of DNA wrapping and DNA bending defective mutants on subunit exchange. (**a**) 5, 2.5, and 1.25 pmole (triangle indicates increasing dose) of BA.A_{59} and $BA_F.A_{59}$ (as indicated) were incubated in a cleavage assay with 8 pmole of GyrB. (**b**) 2.5, 1.25, and 0.625 pmole (triangle indicates increasing dose) of BA.A_{59} and $BA_F.A_{59}$ (as indicated) were incubated in a supercoiling assay in the presence of 4 pmole of GyrB. (**c**) 5, 2.5, and 1.25 pmole (triangle indicates increasing dose) of BA.A, BA_FA and BA_G.A were incubated in a cleavage assay in the presence of 8 pmole of GyrB. (**d**) 2.5, 1.25, and 0.625 pmole (triangle indicates increasing dose) of BA.A_{59} and $BA_F.A_{59}$ (as indicated) were incubated in a supercoiling assay in the presence of 4 pmole of GyrB. Omitting GyrB from all these assays abolished either the supercoiling or cleavage respectively. The exception being BA.A_{59}, which shows a small amount of double-strand cleavage in the absence of GyrB (***Figure 6—figure supplement 1***).

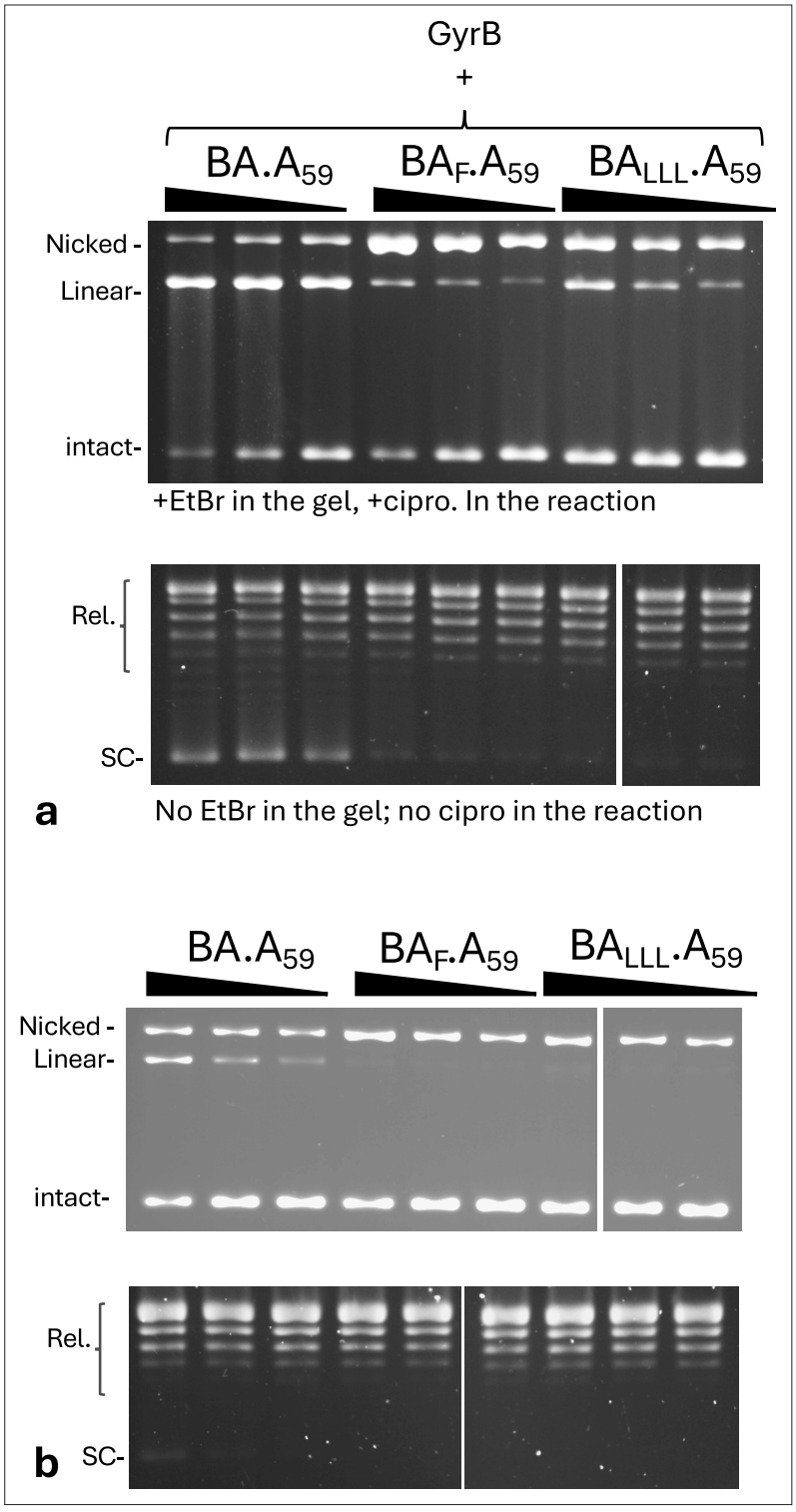

Figure 6—figure supplement 1. Cleavage and supercoiling activity of various heterodimer mutants. (**a**) Cleavage and supercoiling activity of various heterodimer mutants, lacking a CTD. Top. 5, 2.5, and 1.25 pmole (triangle indicate increasing dose) of $BA.A_{59}$, $BA_{F}.A_{59}$, and $BA_{LLL}.A_{59}$ were incubated in a cleavage assay in the presence of GyrB. $BA_{LLL}.A_{59}$ displays significantly more double-strand to single-strand cleavage compared to $BA_{F}.A_{59}$. Bottom. 1.25, 0.625, and 0.312 pmole pmole of $BA.A_{59}$, $BA_{F}.A_{59}$, and $BA_{LLL}.A_{59}$ were tested in a supercoiling assay in the presence of GyrB. (**b**) Top. Cleavage assay, as above, in the absence of GyrB. Bottom. Supercoiling assay, as above, in the absence of GyrB.

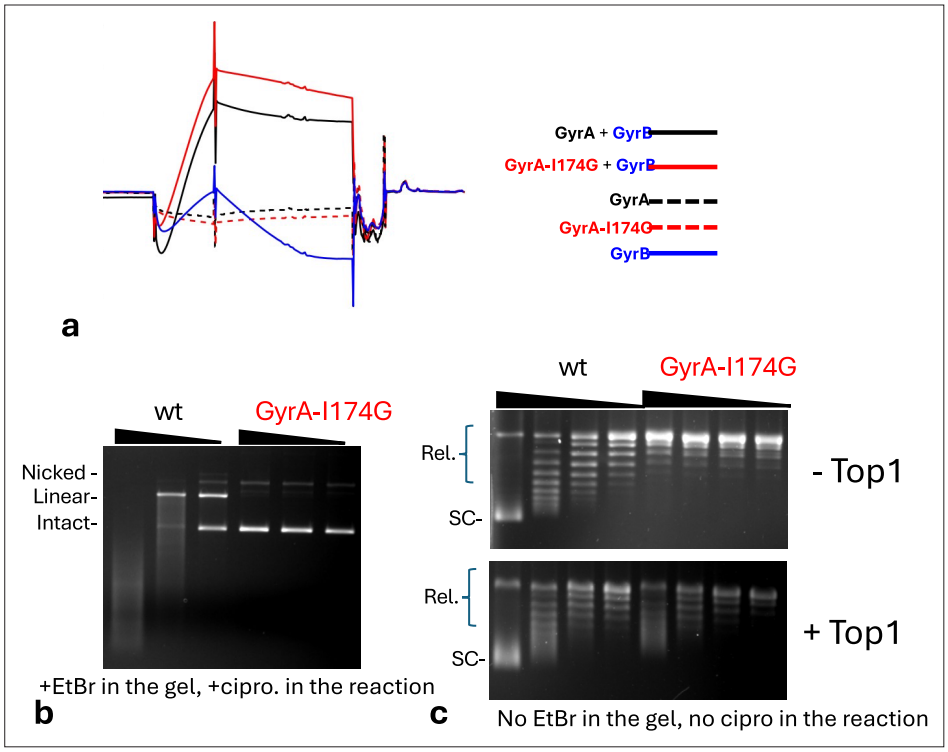

Figure 6—figure supplement 2. Analysis of cleavage and DNA binding properties of the GyrA-I174G mutant homodimer. (**a**) Surface Plasmon Resonance performed with a 170 bp DNA fragment immobilized on a SPR chip. Various preparations were flowed on to the chip, as indicated, and the response recorded. GyrA dimers (wild-type and mutant) showed no binding on their own. GyrB showed limited binding. GyrA and GyrB in combination displayed a strong response, showing robust binding. The concentration of GyrA dimers and GyrB were identical between experiments. (**b**) Cleavage activity of wild-type GyrA and GyrA-I174G. Increasing amounts (triangle) of GyrA dimers as indicated were incubated in the presence of GyrB and 20 μM ciprofloxacin. The I174G mutation abolished cleavage. Supercoiling activity is also abolished (not shown). (**c**) Topological footprint of GyrA wild type and mutant. Increasing amounts of GyrA (triangle) were incubated, in the absence of ATP and ciprofloxacin, with relaxed plasmid DNA and GyrB. *E. coli* Top1 was then added to relax free supercoiling, deproteinization reveals the positive supercoiling constrained by the enzyme. Wild type gyrase can relax DNA, and therefore constrained positive supercoils are visible in the absence of Top1. GyrA-I174G has lost cleavage activity and therefore relaxation activity but can still constrains a limited number of positive supercoils. The handedness of supercoils was ascertained by running agarose gels in the presence of chloroquine (not shown).

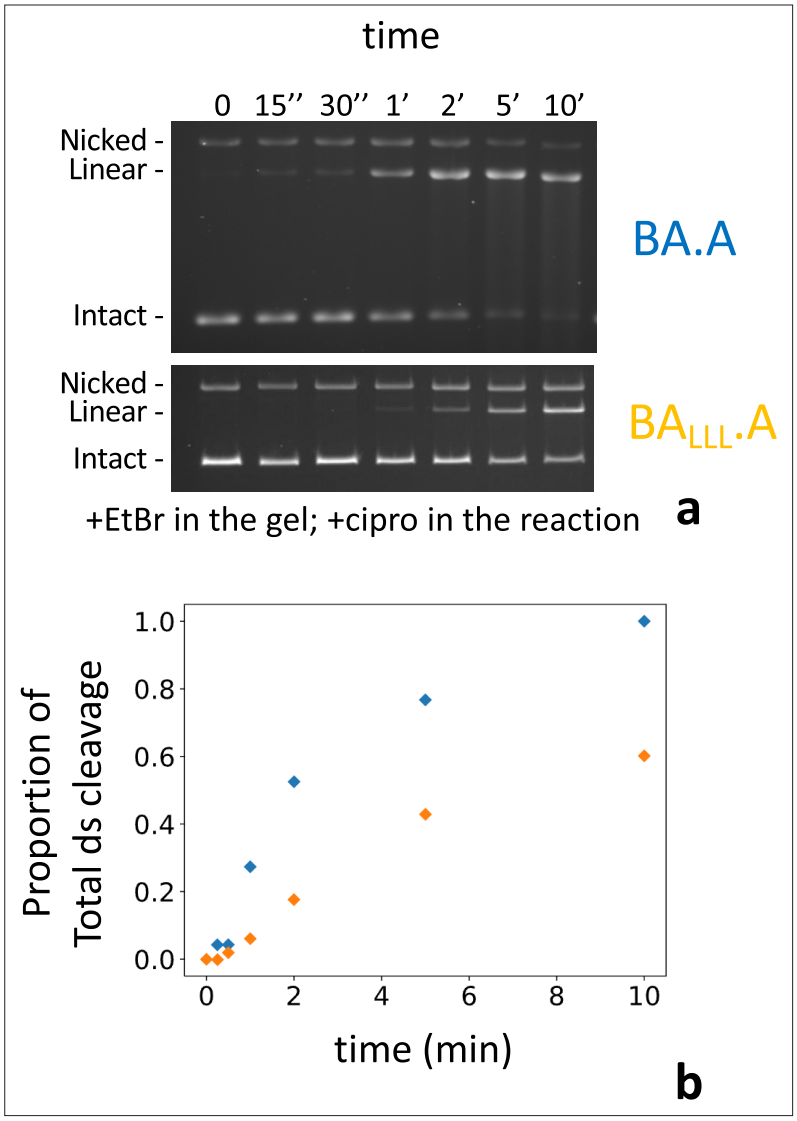

Figure 7. Kinetics of subunit exchange. (**a**) Five pmole of either BA.A (blue) or BA_{LLL}.A (orange) were incubated with 8 pmole of GyrB in a cleavage assay for the indicated times. BA_{LLL}.A +GyrB reaches a level of cleavage comparable to BA.A (albeit much later, around 60 min, not shown). (**b**) Quantification of the gels shown in (**a**). The proportion of linear of the total amount of material in each lane is plotted against time. The proportion of linear is normalized as the fraction of the total amount of linear reached at 60 min, minus background cleavage (low in that instance) observed at the 0 time point.

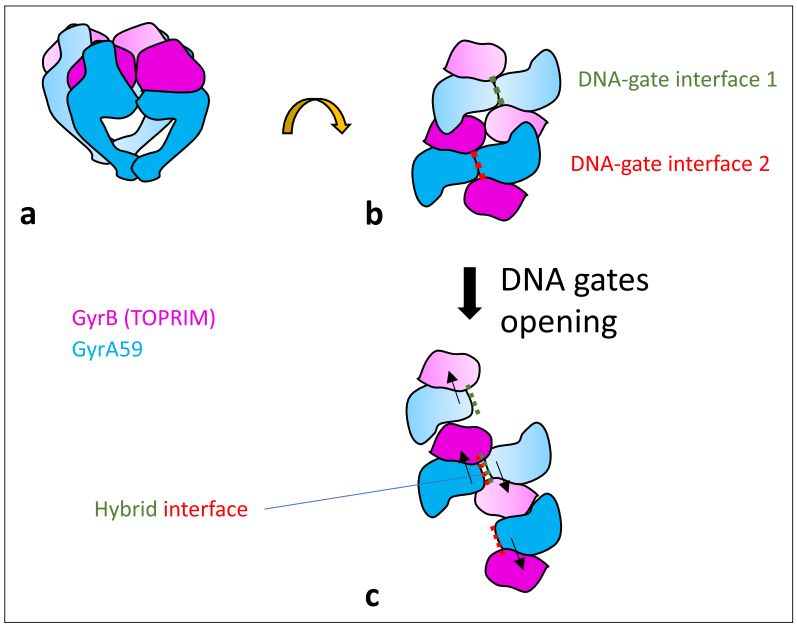

Figure 8. Proposed model for interface swapping. (**a**) Cartoon schematic of two gyrase complexes in close proximity, viewed from the side. Only the core complex is shown. (**b**) 90° rotation view. The gyrase 'super-complex' is viewed from the top. (**c**) The opening of each DNA-gate interface occurs by a sliding movement (black arrows), allowing reformation of a hybrid interface, in the center of the super-complex. The DNA is not represented.

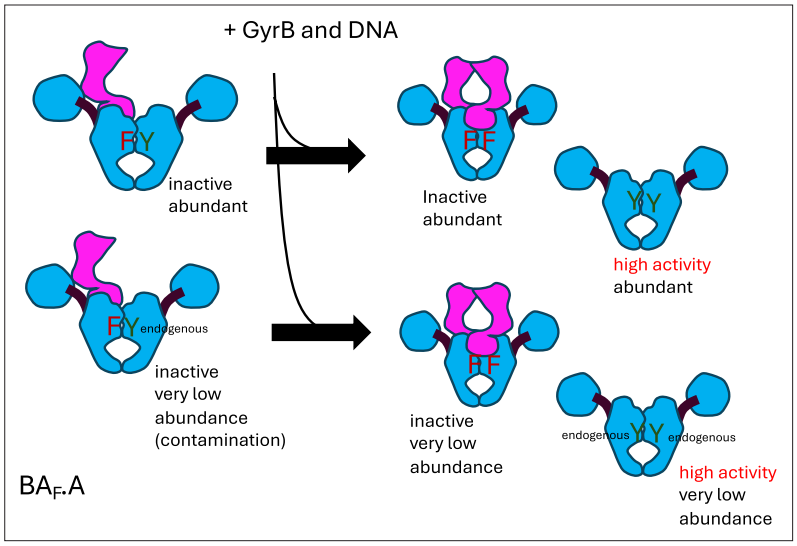

Figure 8—figure supplement 1. Schematic of possible sequential interface swapping mechanism leading to complete subunit exchange for the BA$_F$.A preparation. Only complete subunit exchange is shown. The phenylalanine that replaces the catalytic tyrosine is shown in dark red. The estimated activity and abundance of each product is shown. This preparation is therefore expected to have an overall high supercoiling activity and high cleavage activity.

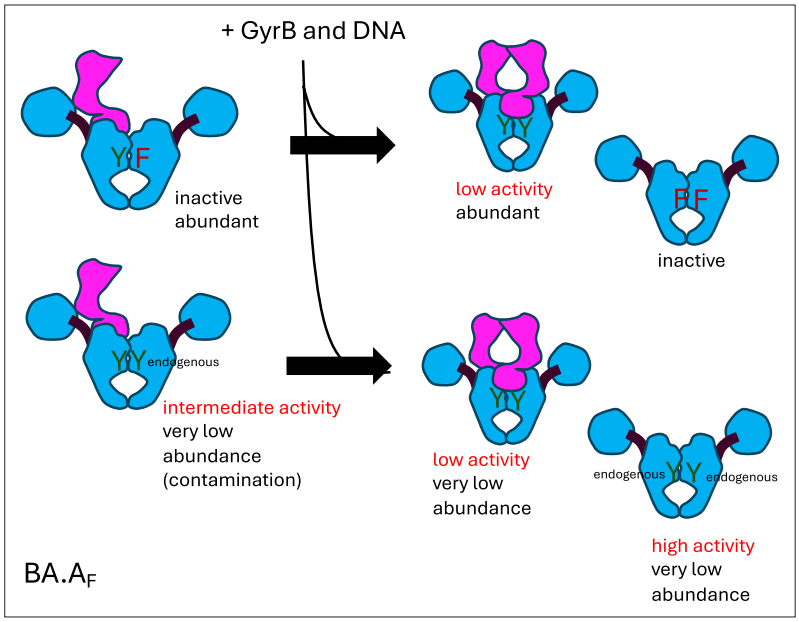

Figure 8—figure supplement 2. Schematic of possible sequential interface swapping mechanism leading to complete subunit exchange for the BA.A$_F$ preparation. Only complete subunit exchange is shown. The phenylalanine that replaces the catalytic tyrosine is shown in dark red. The estimated activity and abundance of each product is shown. This preparation is therefore expected to have an overall low supercoiling activity, low cleavage activity.

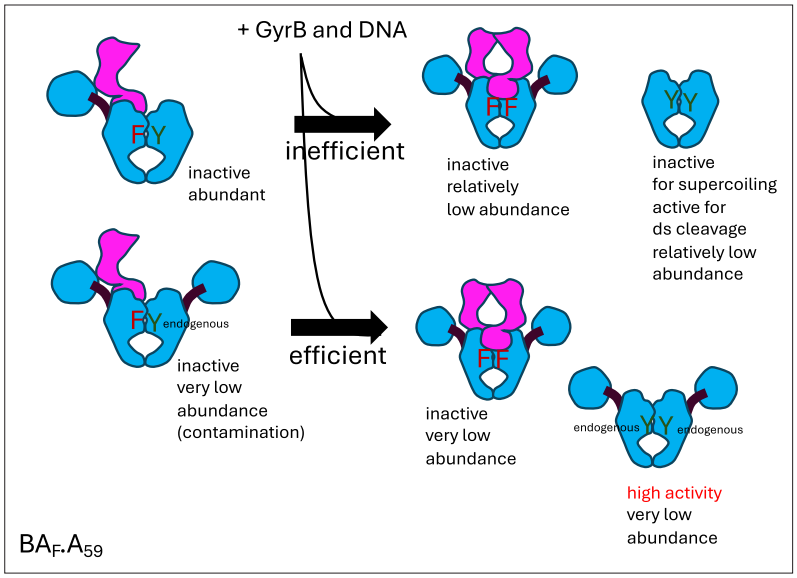

Figure 8—figure supplement 3. Schematic of possible sequential interface swapping mechanism leading to complete subunit exchange for the $BA_{F}.A_{59}$ preparation. Only complete subunit exchange is shown. The phenylalanine that replace the catalytic tyrosine is shown in dark red. The estimated activity and abundance of each product is shown. This preparation is therefore expected to have and overall low supercoiling activity, low cleavage activity.

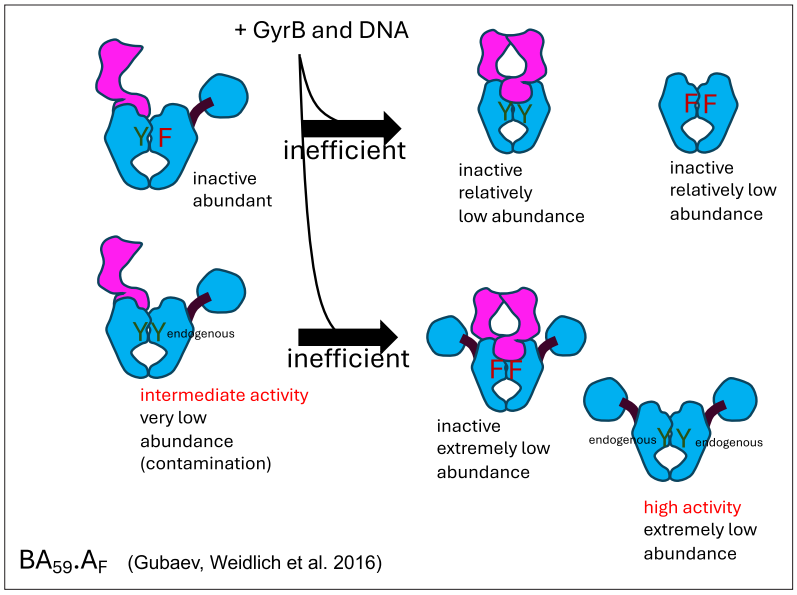

Figure 8—figure supplement 4. Schematic of possible sequential interface swapping mechanism leading to complete subunit exchange for the $BA_{59}.A_F$ preparation. Only complete subunit exchange is shown. The phenylalanine that replaces the catalytic tyrosine is shown in dark red. The estimated activity and abundance of each product is shown. This preparation is therefore expected to have overall very low supercoiling activity and very low cleavage activity.

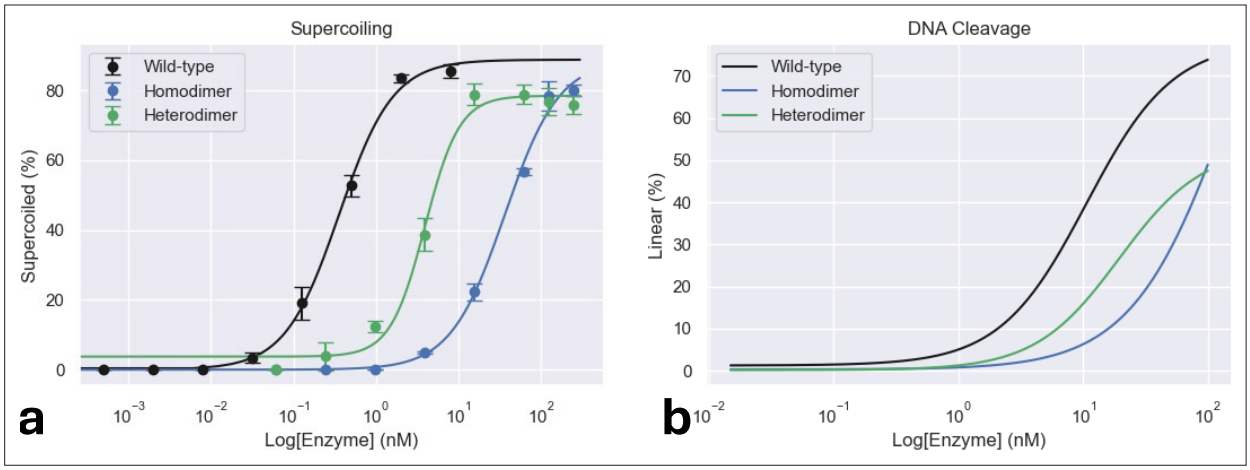

Figure 8—figure supplement 5. Comparison of the activity of the GyrA dimer +free GyrB (wild type), BA.A heterodimer +free GyrB (heterodimer) and $(BA)_2$ (homodimer). (**a**) Supercoiling assay. The IC_{50} (concentration of enzyme producing half the observed supercoiling) is 0.36 nM for the GyrA dimer (wild type), 4 nM for the heterodimer, and 36.7 nM for the $(BA)_2$ homodimer. (**b**) Cleavage assay. The cleavage did not plateau for the heterodimer and $(BA)_2$ homodimer, precluding CC_{50} measurements (concentration of enzyme producing half the maximum level of cleavage).

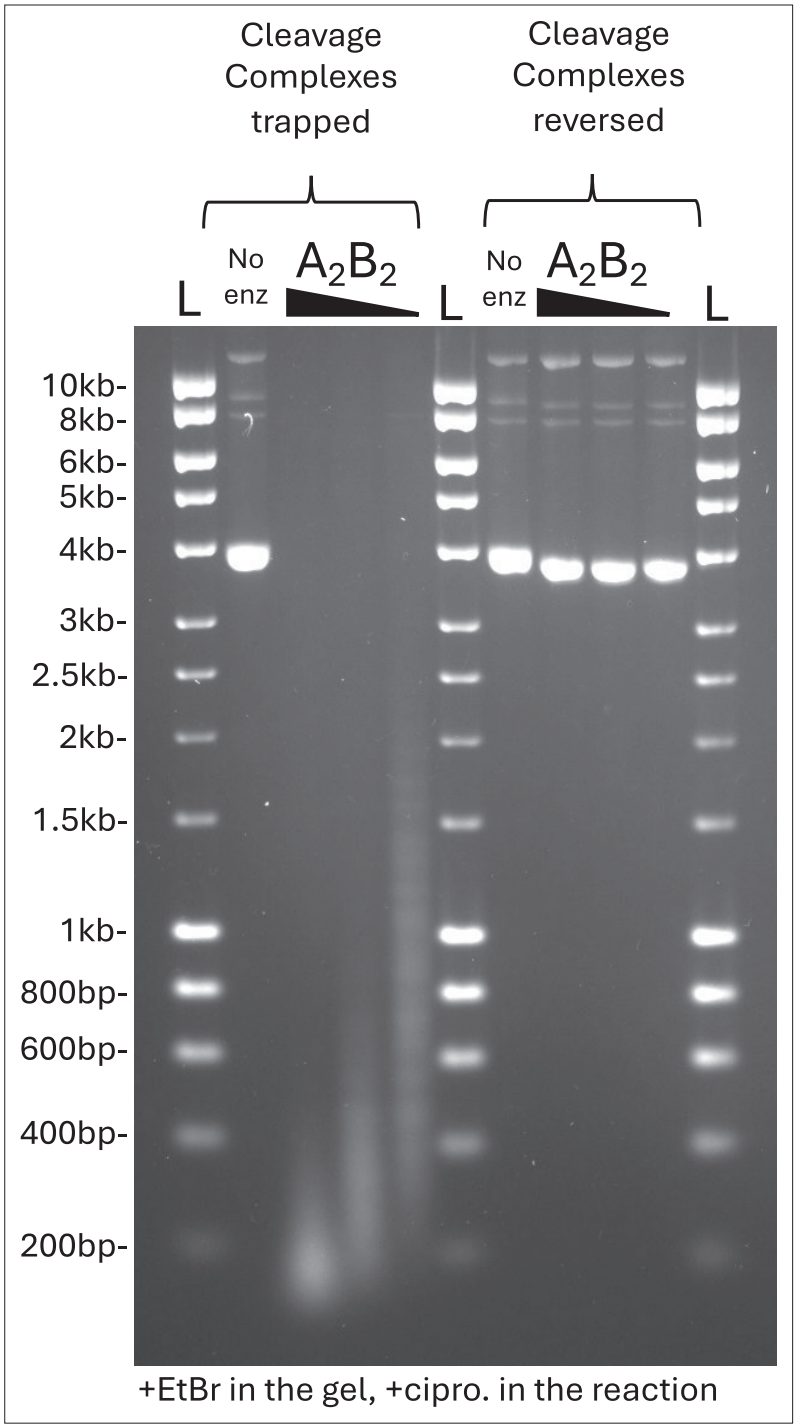

Figure 8—figure supplement 6. Gyrase can stabilize cleavage complexes ~200 bp apart on DNA. A cleavage assay was performed with either no enzyme or 30, 15, and 7.5 pmole of the A_2B_2 tetramer on a~8 kb plasmid (pIRT2tg-NAT), in the presence of 20 μM ciprofloxacin. Cleavages complexes were either trapped by the addition of SDS (methods) or reversed by the addition of EDTA, followed by Proteinase K digestion. The observed cleavage is entirely reversible, showing it arises from the entrapment of genuine cleavage complexes. L: DNA ladder.

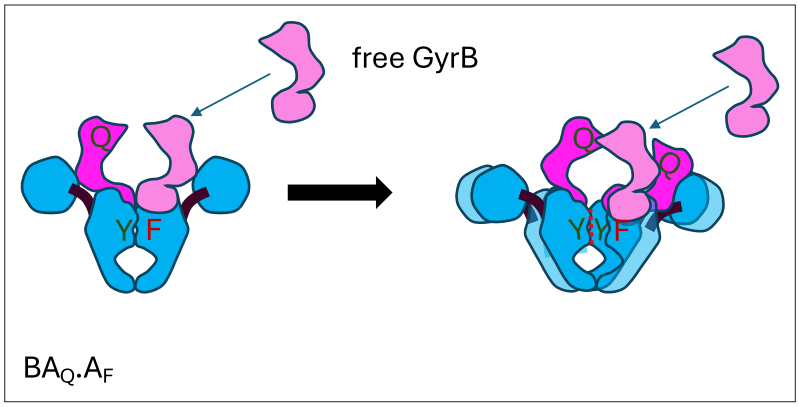

Figure 8—figure supplement 7. Schematic of possible DNA gate-only interface swapping mechanism leading to a $BA_Q.A_F$ preparation having some supercoiling activity in the presence of GyrB. The phenylalanine that replace the catalytic tyrosine is shown in dark red. The free GyrB (light pink) can associate with the $GyrA_F$ subunit and dimerise with $GyrB_Q$ from the BA fusion involved in the exchanged DNA gate interface (red dashed line). The ATPase domain of the other BA_Q fusion involved in the exchanged interface. The TOPRIM domain might not even be exchanged and can still promote cleavage. It is also possible that the whole $GyrB_Q$ domain dissociates from the GyrA domain of the fusion, only staying attached to GyrA at the fusion point; the free GyrB could then replace the fused $GyrB_Q$ and interact with the GyrA domain of the fusion normally. The efficiency of this exchange would presumably depend on the flexibility of the fusion point.